Structural and Improved Dielectric Properties of Bismuth Pyrochlores Containing Interchangeable Ta^{5+} and Nb^{5+} Cations

C. C. Khaw[1,2], P. Y. Tan[3], K. B. Tan[3]*, H. C. Ananda Murthy[4,5], R. Balachandran[6], S. K. Chen[7], O. J. Lee[8] and K. Y. Chan[9]

[1]Department Mechanical and Material Engineering, Lee Kong Chian Faculty of Engineering and Science, Universiti Tunku Abdul Rahman, 43000 Bandar Sungai Long, Kajang, Selangor, Malaysia
[2]Centre for Advanced and Sustainable Materials Research, Universiti Tunku Abdul Rahman, Malaysia
[3]Department of Chemistry, Faculty of Science, Universiti Putra Malaysia, 43400 Serdang, Selangor, Malaysia
[4]Department of Applied Chemistry, School of Natural Science, Adama Science and Technology University, Adama P.O. Box:1888, Ethiopia
[5]Department of Prosthodontics, Saveetha Dental College and Hospital, Saveetha Institute of Medical and Technical Science (SIMATS), Saveetha University, Chennai 600077, Tamil Nadu, India
[6]Department of Electronics and Communication Engineering, Adama Science and Technology University, Adama P.O. Box:1888, Ethiopia
[7]Department of Physics, Faculty of Science, Universiti Putra Malaysia, 43400 Serdang, Selangor, Malaysia.
[8]Faculty of Science and Marine Environment, Universiti Malaysia Terengganu, 21030, Kuala Nerus, Terengganu, Malaysia
[9]Faculty of Engineering, BR4056, Multimedia University, Persiaran Multimedia, 63100, Cyberjaya, Selangor
*Corresponding author (e-mail: tankarban@upm.edu.my)

The pyrochlore structure demonstrates great structural flexibilities, compositional variables, and diverse electrical properties suitable for various electrical applications. This study aimed to synthesise novel pyrochlore phases with improved dielectric performance in the Nb-doped bismuth magnesium tantalate (BMT) system. A complete subsolidus solution was successfully prepared by solid-state reaction through a one-to-one replacement of Ta^{5+} by Nb^{5+} with the proposed chemical formula of $(Bi_{3.50}Mg_{0.50})(Mg_{1.30}Nb_xTa_{2.70-x})O_{13.80}$ ($0.00 \leq x \leq 2.70$). Such doping mechanism implies that both isomorphous Nb^{5+} and Ta^{5+} are highly interchangeable due to their similar crystallo-chemical structures and ionic radii. The incorporation of Nb^{5+} into the BMT host structure resulted in the gradual increase of lattice parameters from 10.5610 (9) to 10.5809 (10) Å. The well-connected polyhedral grains in the range of 2.25–20.00 μm supported their average relative densities of above 80%. The Nb dopant was concluded to significantly enhance the dielectric performance of BMT pyrochlores, i.e., more than two-fold increase of dielectric constant, ε' from 81 to 195, while dielectric loss, tan δ is retained low in the order of 10^{-3}.

Keywords: Pyrochlore; dielectric constant; impedance; niobium

Received: December 2023; Accepted: January 2024

Pyrochlores containing bismuth remain a subject of considerable research interest due to their notable practical advantages, including their excellent dielectric performance, high thermal stability, and compatibility with silver electrode for co-firing at low temperatures. Such characteristics are highly sought after for a wide range of electrical and wireless applications, including but not limited to dielectric ceramic capacitors, low temperature co-fired ceramics (LTCCs), and microwave filters [1-4].

Literally, the pyrochlore structure is denoted by a general formula of $A_2B_2O_6O'$. In this structure, the A-site cations are larger, forming a sublattice of A_2O' with an eightfold coordination. On the other hand, the B-site cations are relatively smaller and occupy the center position of the B_2O_6 octahedra, thus forming an interpenetrating pyrochlore framework through these sublattices. The A cations encompass a wide range of rare earth metals, while the B cations consist of transition metals that exhibit variable oxidation states. The pyrochlore also exhibits a high degree of flexibility with regards to its crystallo-chemical structure, thus allowing substitution of different cations at either A- or B-site, respectively. Meanwhile, the diverse electrical properties ranging from super-conducting to insulating in selected pyrochlore systems also allow them for different functional capabilities [3-7].

Bismuth pyrochlores containing tantalum are still the subject of active research. For instance, $Bi_{1.5}ZnTa_{1.5}O_7$ (BZT) cubic pyrochlore showed ε' of 58, tan δ of 0.0023 at 30°C, and 1 MHz with temperature coefficient of dielectric constant, TCε', of −156 ppm/°C over the range of 30–300°C at 1 MHz.

With careful compositional adjustment, it was possible to achieve a near zero value for its TCε' [8]. Several bismuth tantalate pyrochlore analogues had been reported in our previous studies, including $Bi_{3+5/2x}Mg_{2x}Ta_{3-3/2x}O_{14-x}$ ($0.12 \leq x \leq 0.22$) pyrochlores with ε' in the range of 70–85 and tan δ of 10^{-3} [9], $Bi_{3.36}Fe_{2.08+x}Ta_{2.56-x}O_{14.56-x}$ ($-0.32 \leq x \leq 0.48$) pyrochlores with ε' in the range of ~78–92 and tan δ of $\sim10^{-1}$ [10], as well as the pyrochlores spanned over a broad subsolidus area, $Bi_{2.48+y}Cu_{1.92-x}Ta_{3.6+x-y}O_{14.64+3x/2-y}$ ($0.00(1) \leq x \leq 0.80(1)$ and $0.00\ (1) \leq y \leq 0.60(1)$ that have notable ε' values in the range of ~60–80 and tan δ of ~0.01–0.20 [11]. In other words, these Mg-, Fe- and Cu-analogues have average ε' in the range of ~70–90. Meanwhile, other related studies showed relatively lower values, e.g., ε' of 33–38 and tan δ of ~0.005 for the $Bi_{1.49}Co_{0.8}Ta_{1\cdot6}O_{7.0}$ pyrochlores [12] and ε' of 14–18 and tan δ of ~0.018 for $Bi_{1.6}Cr_{0.8}Ta_{1.6}O_{7\pm\Delta}$ pyrochlores [13], respectively. Typically, bismuth tantalate pyrochlores show weaker dielectric properties if compared to those Nb analogues in the bismuth zinc niobate (BZN) ternary system, whose ε' values are generally more than 100 [2-4, 6, 8]. A number of studies including ours and other researcher groups demonstrated that Nb analogues have better dielectric properties than Ta analogues. $(Bi_{3.36}Mg_{0.64-x}Ca_x)(Mg_{1.28}Nb_{2.72})O_{13.76}$ ($0 \leq x \leq 0.7$) pyrochlores were found to have higher ε' in the range of 69–171 and tan δ of 10^{-3} [14] if compared to $(Bi_{3.36}Mg_{0.64-x}Sr_x)(Mg_{1.28}Nb_{2.72})O_{13.76}$ ($0 \leq x \leq 0.5$) pyrochlores whose ε' of 90–186 and tan δ of $\sim10^{-2}$–10^{-1} [15]. These values are comparable to the reported ε' of 167–204 and tan δ of 10^{-4}–10^{-3} in the undoped $Bi_{3+(5/2)x}Mg_{2-x}Nb_{3-(3/2)x}O_{14-x}$ cubic pyrochlores [16]. In addition, similar dielectric behaviours of Nb analogues were observed by other research groups. The synthesised pyrochlores in the $Bi_{1.5}Mg_{1-x}Na_xNb_{1.5}O_{7-\delta}$ ($x = 0.1$ and 0.25) and $Bi_{1.5}Mg_{0.9-x}Na_xNb_{1.5}O_{7-\delta}$ ($x = 0.25$ and 0.40) systems possessed ε' of 122–153 and tan δ of 0.0025 [17]. Meanwhile, other chemically doped subsolidus pyro-chlores were also prepared successfully, including $Bi_{1.5}Mg_{1-x}Ca_xNb_{1.5}O_7$ ($0 \leq x \leq 0.7$) whose ε' of 86–145 and tan δ of 0.015–0.05 [18] and $Bi_{1.5}Mg_{1-x}Li_xNb_{1.5}O_{7-\delta}$ ($0 \leq x \leq 0.5$) pyrochlore materials that displayed ε' of 86–143 and tan δ of 0.02 [19].

Considering both Ta and Nb cations have an identical ionic radius of 0.64 Å (six-fold coordination) and their crucial characteristic of BO_6 octahedra polarisation, Nb^{5+} was chosen to substitute Ta^{5+} in the bismuth magnesium tantalate (BMT) pyrochlores [2-4, 12-19]. Meanwhile, the electrical performance of functional pyrochlores is also expected to be influenced greatly by the composition variables and the processing control. As such, we undertook a systematic study pertaining to the influence of Nb dopant on BMT pyrochlores, specifically for their subsolidus solubility, structural change, and electrical performance.

EXPERIMENTAL

Preparation of Samples

Samples with the proposed formula of $(Bi_{3.50}Mg_{0.50})(Mg_{1.30}Nb_xTa_{2.70-x})O_{13.80}$ ($0.00 \leq x \leq 2.70$) were prepared by solid-state reaction. The starting materials employed in this study were reagent grade oxide powders, including Bi_2O_3 (Aldrich, 99.99%), MgO (Aldrich, 99%), Nb_2O_5, and Ta_2O_5 (Alfa Aesar, 99.9%). Pre-heat treatment was performed for Bi_2O_3 at 300°C and MgO, Ta_2O_5 and Nb_2O_5 at 600°C, respectively. The stoichiometric amounts of the oxides were weighed out and pulverised using an agate mortar and pestle in adequate reagent grade acetone. During the initial stage, the mixtures were carefully transferred into a platinum boat prior to calcination in a muffle furnace. A step-wise firing procedure was applied, including firings at 300°C and 600°C for 1 hour before 800°C overnight. This promoted the formation of low temperature intermediates to avoid loss of bismuth and to allow subsequent firing at high temperatures. Lastly, the firing was completed at 1025°C for 48 h, wherein the thermal equilibrium was also confirmed through a prolonged heating and/or higher temperatures. Notably, the powders were subjected to intermittent regrinding to enhance their homogeneity by bringing more fresh surface area. Then, these powders were cold pressed into pellets of 8 mm in diameter and ~2–3 mm in thickness by a uniaxial hydraulic press. The applied densification at 1075°C for 24 h led to the attainment of relative densities above 80%.

Sample Characterisation

The phase purity of the prepared samples was confirmed using an automated Shimadzu 6000 X-ray diffractometer equipped with CuKα radiation of 1.5406 Å. The X-ray diffraction (XRD) data obtained at a scan rate of 1.0°/min were utilised for the lattice refinement using Chekcell programme. A scanning electron microscope (SEM, JOEL JSM-6400) was utilised to study the surface morphology of the gold sputtered sample pellets. Elemental analyses were performed through an ICP-OES spectrometer (Perkin Elmer Optima 2000DV) using sample triplicates in 5% hydrofluoric acid and blank solution of 5% nitric acid. The densified pellets were coated with gold electrodes prior to the electrical measurement using an AC impedance analyser, Hewlett-Packard HP4192A in the frequency range of 5 Hz–13 MHz. The electrical data were taken during a heat-cool cycle over the temperature range of 30-850°C, following a 25-minute equilibration time. The electrical data were normalised by the geometric factors of pellets and corrected for the stray capacitance of the empty jig.

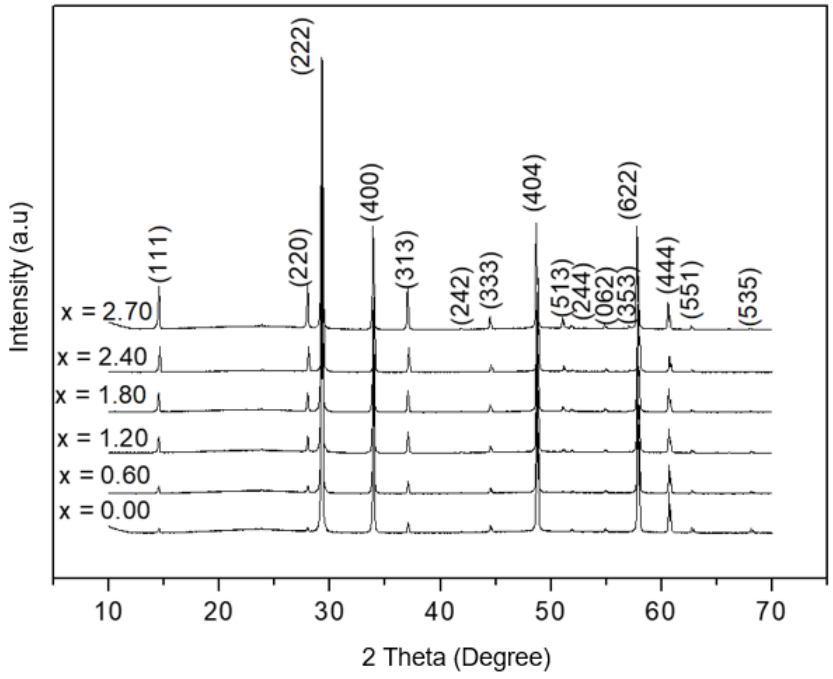

Figure 1. XRD patterns of $(Bi_{3.50}Mg_{0.50})(Mg_{1.30}Nb_xTa_{2.70-x})O_{13.80}$ $(0.00 \leq x \leq 2.70)$ pyrochlores as a function of dopant concentration.

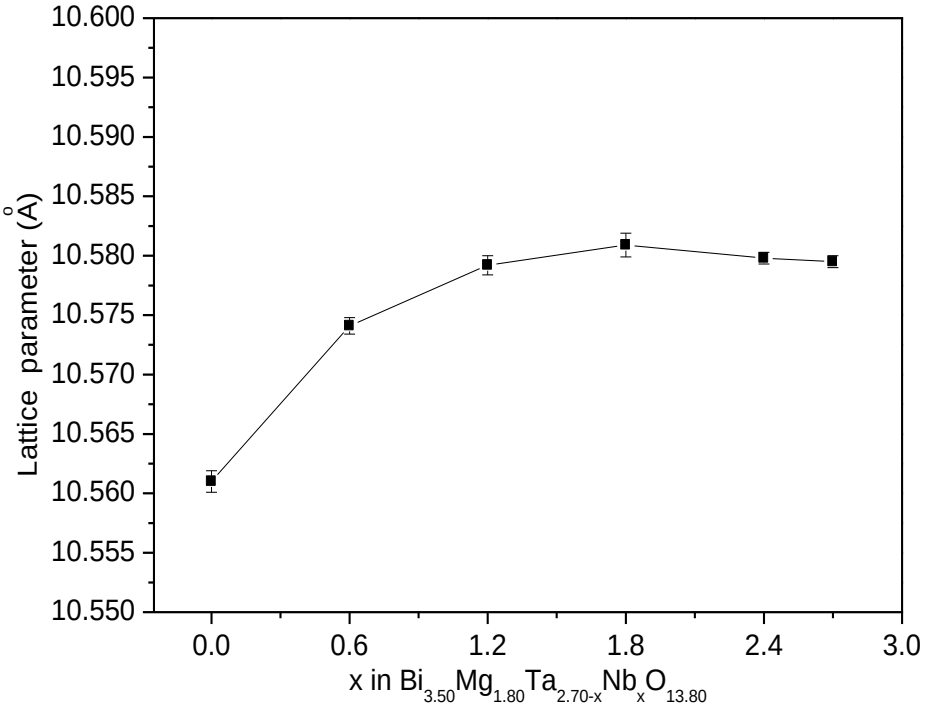

Figure 2. Lattice parameters of $(Bi_{3.50}Mg_{0.50})(Mg_{1.30}Nb_xTa_{2.70-x})O_{13.80}$ $(0.00 \leq x \leq 2.70)$ pyrochlores as a function of dopant concentration.

RESULTS AND DISCUSSION

X-Ray Diffraction (XRD) Analysis

Figure 1 shows the XRD patterns for Nb-substituted $(Bi_{3.50}Mg_{0.50})(Mg_{1.30}Nb_xTa_{2.70-x})O_{13.80}$ $(0.00 \leq x \leq 2.70)$ pyrochlores. The XRD patterns did not exhibit any discernible secondary phases wherein the Ta cations could be replaced completely by Nb cations in the host structure. This demonstrates that a complete range of solid solutions was formed through a one-to-one homovalent substitution. A similar observation was

observed in Ta-doped bismuth zinc niobate (BZN) pyrochlores, $Bi_{1.5}Zn_{0.92}Nb_{1.5-x}Ta_xO_{6.92}$ wherein their solid solution limit was determined to be 0.0 to 1.5 [20]. This implies that the isomorphous characteristic and identical ionic radii of 0.64 Å (six-fold coordination) for both Ta and Nb cations have rendered them highly interchangeable. The entire Nb-doped bismuth magnesium tantalate (BMT) pyrochlores are well crystallised in a cubic structure with the space group of *Fd3m*, No. 227. All the diffraction planes could be fully indexed, thus confirming these chemically doped pyrochlores are phase pure by XRD analysis [8, 20]. Figure 2 shows the variation of lattice parameters of Nb-doped materials with composition, x. These Nb-doped materials showed a progressive unit cell expansion with higher Nb concentration, reaching a maximum at x = 1.80; however, these values remained relatively constant thereafter. It has been postulated that the relaxation involving the central ion in BO_6 octahedra may be caused by the greater polarisability of Nb in comparison to Ta [7-9]. Subsequently, the variation in bond length may lead to a marginal larger unit cell. The lattice parameters of all the Nb-doped BMT pyrochlores fell within the range of 10.5610 (9) – 10.5809 (10) Å.

Elemental Analysis

ICP-OES was utilised to ascertain the elemental concentrations (excluding O) of the Nb-doped BMT pyrochlores, which were then expressed as atomic percentages. Oxygen content was determined by the difference between cationic concentrations from the prepared sample triplicates. Table 1 provides a summary of the determined atomic percentages of the elements. The observed values are closely aligned with the theoretical concentrations, i.e., less than 5% of the permissible error. This supports the absence of any discernible systematic deviation from the chemical stoichiometry, specifically no indication of substantial Bi_2O_3 loss during high temperature firing.

Table 1. Elemental analysis of Nb-doped BMT pyrochlores.

Sample	Elements	Atomic %		Number of Atom	
		Calculated	Experimental	Calculated	Experimental
$Bi_{3.50}Mg_{1.80}Ta_{2.10}Nb_{0.60}O_{13.80}$	Bi	16.06	14.90±0.05	3.50	3.33±0.01
	Mg	8.26	9.07±0.15	1.80	2.03±0.03
	Ta	9.63	9.94±0.15	2.10	2.22±0.03
	Nb	2.75	2.79±0.40	0.60	0.62±0.08
	O	63.30	63.30±1.71	13.80	14.15±0.37
$Bi_{3.50}Mg_{1.80}Ta_{1.50}Nb1_{.20}O_{13.80}$	Bi	16.06	14.28±0.09	3.50	3.35±0.02
	Mg	8.26	9.56±0.046	1.80	2.25±0.01
	Ta	6.88	5.52±0.03	1.50	1.30±0.01
	Nb	5.51	6.83±0.06	1.20	1.60±0.01
	O	63.30	63.81±1.88	13.80	14.99±0.41
$Bi_{3.50}Mg_{1.80}Ta_{0.90}Nb_{1.80}O_{13.80}$	Bi	16.06	15.52±0.27	3.50	3.40±0.06
	Mg	8.26	10.26±0.09	1.80	2.24±0.02
	Ta	4.13	4.37±0.03	0.90	0.96±0.01
	Nb	8.26	8.59±0.04	1.80	1.88±0.01
	O	63.30	61.27±3.79	13.80	13.40±0.83
$Bi_{3.50}Mg_{1.80}Ta_{0.30}Nb_{2.40}O_{13.80}$	Bi	16.06	16.73±0.03	3.50	3.49±0.01
	Mg	8.26	10.88±0.06	1.80	2.27±0.01
	Ta	1.38	1.54±0.01	0.30	0.32±0.01
	Nb	11.01	12.11±0.11	2.40	2.53±0.02
	O	63.30	58.75±0.97	13.80	12.26±0.21

Table 2. Calculated grain sizes, crystallite sizes and internal strains of BMT pyrochlores.

x	C_{size} = average crystallite size		W-H plot strain, ε ($x10^{-4}$)	Grain size (μm)
	Scherrer (nm)	W-H method		
0.00	68	41	6.5	2.50-10.00
0.60	58	36	7.3	0.80-10.40
1.20	52	32	8.5	1.20-14.00
1.80	61	36	7.3	2.00-20.00
2.40	75	45	5.8	4.80-20.00
2.70	78	50	5.8	2.25-8.75

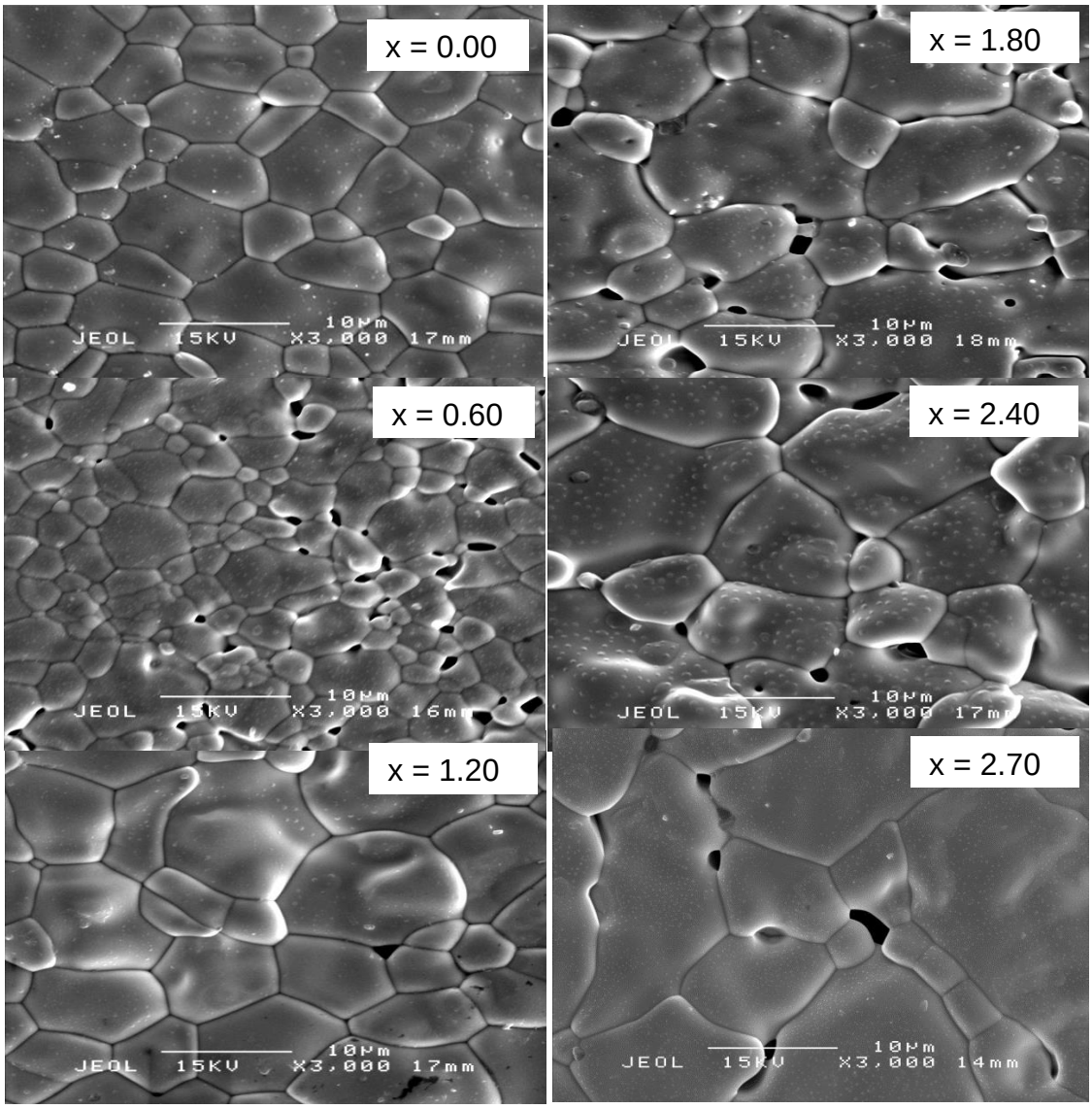

Figure 3. SEM micrographs of $(Bi_{3.50}Mg_{0.50})(Mg_{1.30}Nb_xTa_{2.70-x})O_{13.80}$ ($0.00 \leq x \leq 2.70$) Pyrochlores.

Surface Morphology Study

The SEM micrographs of the Nb-doped BMT pyrochlores are illustrated in Figure 3. These ceramics consisted of polyhedral grains with their sizes ranging from 0.80 to 20.00 μm. The calculations for crystallite size of the Nb-doped BMT pyrochlores were performed by both Williamson-Hall and Scherrer methods. The crystallite size values for these approaches differed marginally wherein a similar trend was observed, as

shown in Figure 4. This is because the determination of crystallite size by the Williamson-Hall method covers multiple intense X-ray diffraction peaks and internal strain of structure, as illustrated in Figure 5. On the contrary, only the most intense X-ray diffraction peak is taken into consideration for the latter method. The extremely small strains, in the order of 10^{-4}, indicate that the substituted Nb dopants has an insignificant impact on the pyrochlore structure. The XRD patterns also did not exhibit any significant peak broadening and/or satellite peak related to the lattice ordering of superstructure. Thus, the Nb-doped BMT pyrochlores were free of any cell distortion. The grain size, crystallite size, and strain values of the Nb-doped BMT pyrochlores are summarised in Table 2.

Electrical Properties

Figure 6 shows the Arrhenius conductivity plots of the Nbdoped BMT pyrochlores. The bulk resistance of these materials was extracted from the perfect semicircles obtained from the Cole-Cole plots. The results reveal that the conductivity of these samples increases as the temperature rises. Also, there was no systematic shift in conductivity with increasing Nb dopant concentration. The activation energies of

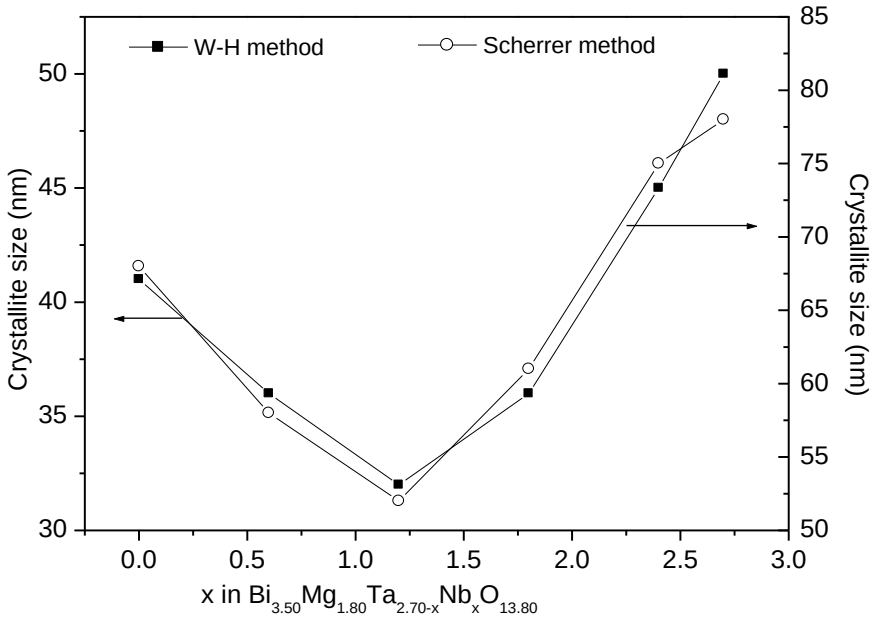

Figure 4. Crystallite size analysis of Nb-doped BMT pyrochlores.

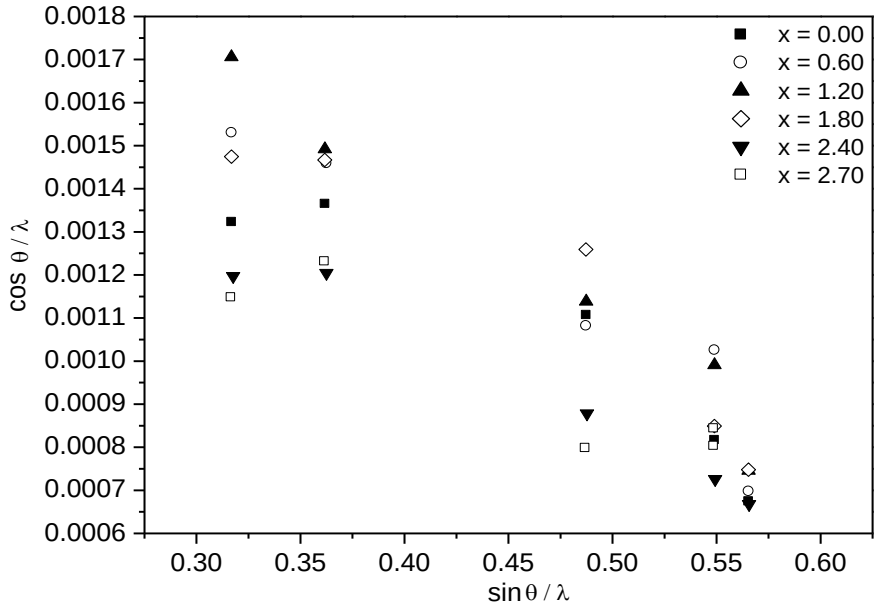

Figure 5. Williamson-Hall plots of Nb-doped BMT pyrochlores.

these Nb-doped BMT pyrochlores fell in the range of 1.14 and 1.51 eV, with the highest value obtained for composition, x = 1.20. Literally, the electronic hopping process is responsible for the high activation energy, i.e., ≥ 1.0, when it is not linked to the ionic conduction mechanism [8-11]. The incorporation of Nb dopant into BMT pyrochlores resulted in the increase of ε' (Figure 7). At room temperature and fixed frequency of 1 MHz, the Nb-doped BMT pyrochlores had the lowest ε' of 81 when x = 0.00 and the highest ε' value of 195 when x = 2.70. Such observations show a systematic change of ε' consistent with the increasing dopant concentration. The increase in ε' could be explained by an increase of the total polarisability of the pyrochlore structure, as the magnitude of ε' depends on the degree of the polarisation or cationic displacement. In addition, the lower ε' might be due to a stronger polarisation in NbO_6 octahedra compared to that of relatively weaker TaO_6 octahedra [8, 21].

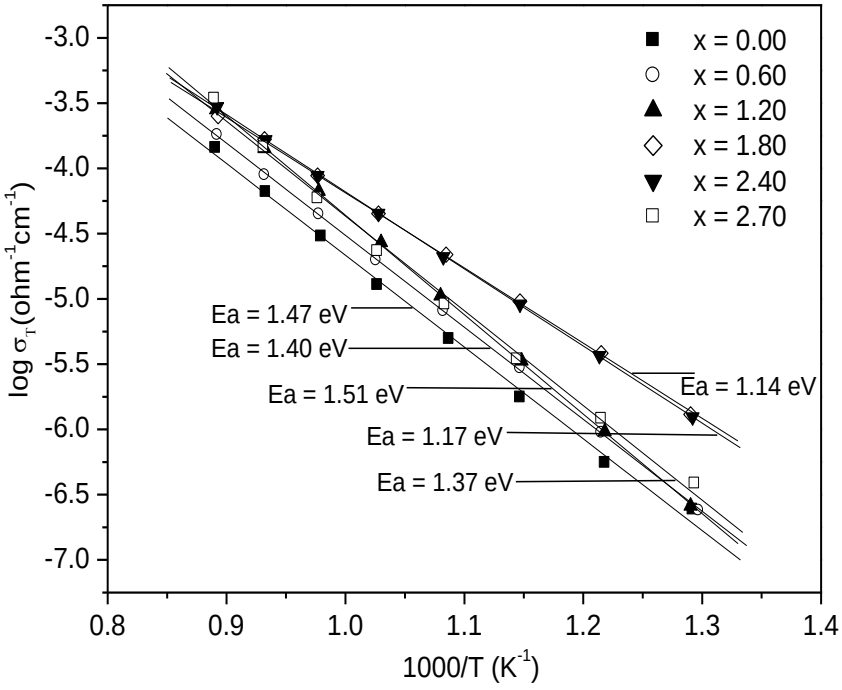

Figure 6. Arrhenius conductivity plots of Nb-doped BMT pyrochlores.

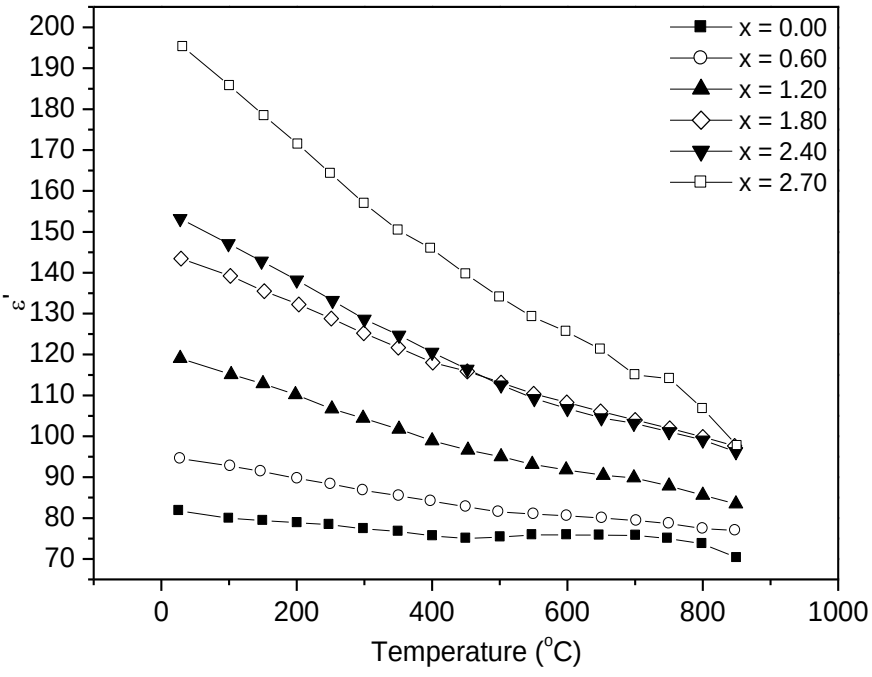

Figure 7. ε' of Nb-doped BMT pyrochlores as a function of temperature.

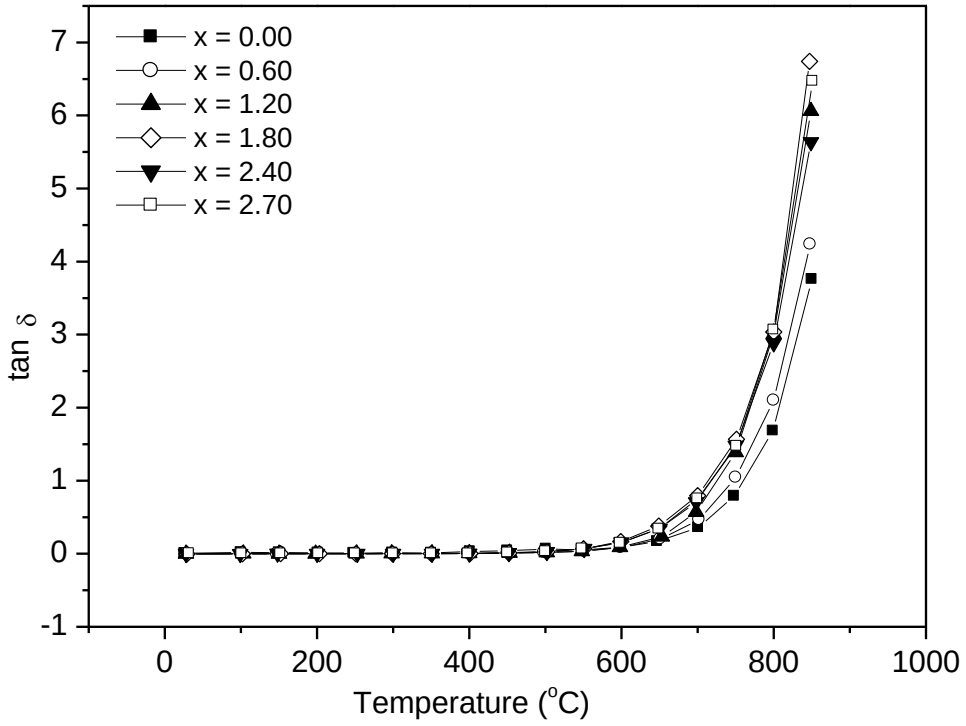

Figure 8. Tan δ of Nb-doped BMT pyrochlores as a function of temperature

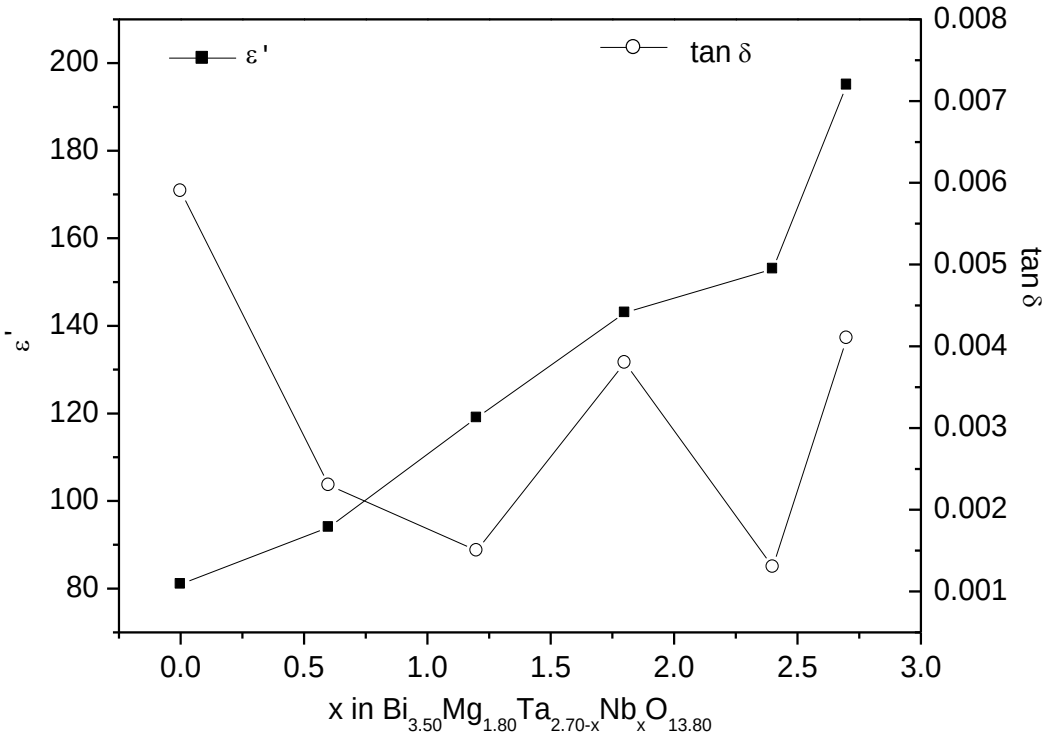

Figure 9. ε' and tan δ of Nb-doped BMT pyrochlores as a function of dopant concentration.

Table 3. Summary of electrical properties of Nb-doped BMT pyrochlores.

Composition x	Dielectric constant, ε'	Dielectric loss, tan δ	Temperature coefficient of dielectric constant, TCε' (ppm/°C) ~30°C - 300°C	Activation energy, Ea (eV)
0.00	81	0.0059	-197	1.47
0.60	94	0.0023	-302	1.40
1.20	119	0.0015	-454	1.51
1.80	143	0.0038	-471	1.14
2.40	153	0.0013	-590	1.17
2.70	195	0.0041	-742	1.37

It was noticeable that the TCε' of the Nb-doped BMT pyrochlores increases as the Nb content increases, with values ranging from - 197 to 742 ppm/°C. Similar results were observed in Ta-doped BZN pyrochlores, $Bi_{1.5}Zn_{0.92}Nb_{1.5-x}Ta_xO_{6.92}$ wherein higher Ta contents had resulted in a drastic drop of TCε' from - 760 ppm/°C in the pure BZN to - 190 ppm/°C at x = 1.5 [20]. In a chemically substituted α-BZN system, Valent and Davies [4] proposed a correlation between TCε' and the ratio of the A- and B-site ionic radii (r_A/r_B), i.e., increasing TCε' with smaller ratio value of r_A/r_B. It is unlikely applicable to the case of Nb-doped BMT pyrochlores, though, because both interchangeable Nb^{5+} and Ta^{5+} have identical ionic radii of 0.64 Å. Nonetheless, it is apparent that the replacing Nb^{5+} ions should be the origin of TCε' value change. The relatively higher polarisable Nb^{5+} than the replaceable ions, Ta^{5+} may cause the off-centring displacement owing to the possible cationic loosening at the centre of BO_6 octahedra [22]. Consequently, this may result in different bond lengths and bond strengths, affecting the TCε' values of chemically modified BMT pyrochlores, accordingly.

Figure 8 shows tan δ as a function of temperature at the fixed frequency of 1 MHz. Tan δ of the samples was found to be temperature-independent at temperatures below 600°C. However, an abrupt increase in tan δ was observed at temperatures above 600°C. This phenomenon is due to the increase of thermally activated drift mobility of charge carriers according to the hopping conduction [8-11]. The Nb-doped BMT pyrochlores retained low tan δ in the order of 10^{-3}, specifically in the range of 0.0013 – 0.0059, indicating that the Nb dopants had a negligible effect. Figure 9 shows ε' and dielectric loss with the variation of x at room temperature and the frequency of 1 MHz. The summary of electrical properties of the Nb-doped materials is shown in Table 3.

CONCLUSION

The successful incorporation of Nb_2O_5 into the pyrochlore host structure has resulted in a complete subsolidus solution, wherein these BMT pyrochlores could be well described by the chemical formula of $(Bi_{3.50}Mg_{0.50})(Mg_{1.30}Nb_xTa_{2.70-x})O_{13.80}$ ($0.00 \leq x \leq 2.70$). These Nb-doped BMT pyrochlores exhibited moderate high activation energy in the range of 1.17–1.51 eV. A significant improvement in ε' with increasing Nb dopant concentration was observed, while low tan δ could be retained in the order of 10^{-3}. The change in ε' is postulated to be closely associated with the higher degree of BO_6 polarisation due to the Nb substitution. Such high bulk ε' and low tan δ suggest these Nb-doped BMT pyrochlores could serve as alternative candidates for the application in multi-layered cofired ceramics.

ACKNOWLEDGEMENT

Special thanks to the Ministry of Higher Education, Malaysia for the financial support via Fundamental Research Grant Scheme (FRGS- 01-01-20-2304).

REFERENCES

1. Sales, A. J. M., Melo, B. M. G., Teixera, S. S., Devesa, S., Oliviera, R. G. M., Oliviera, P. W. S, Vasconcelos, S. J. T., Graca, M. P. F., Costa, L. C. and Sombra, A. S. B. (2021) Influence of pyrochlore phase on the dielectric properties of the bismuth niobate system. *Materials Science and Engineering B*, **263**, 114880.

2. Guo, Q., Li, L., Yu, S., Sun, Z., Zheng, H., Li, J. and Luo, W. (2018) Temperature–stable dielectrics based on Cu–doped $Bi_2Mg_{2/3}Nb_{4/3}O_7$ pyrochlore ceramics for LTCC. *Ceramics International*, **44(1)**, 333–338.

3. Yu, S., Li, L. and Zheng, H. (2017) BMN-based transparent capacitors with high dielectric tunability. *Journal of Alloys and Compounds*, **699**, 68–72.

4. Valant, M. and Davies, P. K. (2000) Crystal chemistry and dielectric properties of chemically substituted $(Bi_{1.5}Zn_{1.0}Nb_{1.5})O_7$ and $Bi_2(Zn_{2/3}Nb_{4/3})O_7$

pyrochlores. *Journal of American Ceramic Society*, **83(1)**, 147–153.

5. Subramanian, M. A., Aravamudan, G. and Rao, G. V. S. (1983) Oxide pyrochlores - a review. *Progress in Solid State Chemistry*, **15(2)**, 55–143.

6. Hong, W., Huiling, D. and Xi, Y. (2003) Structural study of Bi_2O_3-ZnO-Nb_2O_5 based pyrochlores. *Materials Science and Engineering B*, **99(1)**, 20–24.

7. Miles, G. C. and West, A. R. (2006) Pyrochlore phases in the system ZnO-Bi_2O_3-Sb_2O_5: I. stoichiometries and phase equilibria. *Journal of American Ceramic Society*, **89(3)**, 1042–1046.

8. Khaw, C. C., Tan, K. B. and Lee, C. K. (2009) High temperature dielectric properties of cubic bismuth zinc tantalate. *Ceramics International*, **35(4)**, 1473–1480.

9. Tan, P. Y, Tan, K. B., Khaw, C. C., Zainal, Z., Chen, S. K. and Chon, M. P. (2012) Structural and electrical properties of bismuth magnesium tantalate pyrochlores. *Ceramics International*, **38(7)**, 5401–5409.

10. Jusoh, F. A., Tan, K. B., Zainal, Z., Chen, S. K., Khaw, C. C. and Lee, O. J. (2020) Novel pyrochlores in the Bi_2O_3-Fe_2O_3-Ta_2O_5 (BFT) ternary system: synthesis, structural and electrical properties. *Journal of Materials Research and Technology*, **9(5)**, 11022–11034.

11. Chon, M. P., Tan, K. B., Khaw, C. C., Zainal, Z., Taufiq-Yap, Y. H., Chen, S. K. and Tan, P. Y. (2016) Subsolidus phase equilibria and electrical properties of pyrochlores in the Bi_2O_3–CuO–Ta_2O_5 ternary system. *Journal of Alloys and Compounds*, **675**, 116–127.

12. Zhuk, N. A., Krzhizhanovskaya, M. G., Sekushin, N. A., Sivkov, D. V. and Abdurakhmanov, I. E. (2023) Crystal structure, dielectric and thermal properties of cobalt doped bismuth tantalate pyrochlore. *Journal of Materials Research and Technology*, **22**, 1791–1799.

13. Zhuk, N. A, Sekushin, N. A, Krzhizhanovskaya, M. G., Koroleva, A. V., Reveguk, A. A., Nekipelov, S. V., Sivkov, D. V., Lutoev, V. P., Makeev, B. A., Kharton, V. V., Lebedev, A. M., Chumakov, R. G., Koksharova, K. D. and Shpynova, A. D. (2023) Cr-doped bismuth tantalate pyrochlore: Electrical and thermal properties, crystal structure and ESR, NEXAFS, XPS spectroscopy. *Materials Research Bulletin*, **158**, 112067.

14. Dasin, N. A. M., Tan, K. B., Khaw, C. C., Zainal, Z., Lee, O. J. and Chen, S. K. (2020) Doping mechanisms and dielectric properties of Ca-doped bismuth magnesium niobate pyrochlores. *Materials Chemistry and Physics*, **242**, 122558.

15. Dasin, N. A. M., Tan, K. B., Khaw, C. C., Zainal, Z. and Chen, S. K. (2017) Subsolidus solution and electrical properties of Sr-substituted bismuth magnesium niobate pyrochlores. *Ceramics International*, **43(13)**, 10183–10191.

16. Tan, P. Y, Tan, K. B., Khaw, C. C., Zainal, Z., Chen, S. K. and Chon, M. P. (2014) Phase equilibria and dielectric properties of $Bi_{3+(5/2)x}Mg_{2-x}Nb_{3-(3/2)x}O_{14-x}$ cubic pyrochlores. *Ceramics International*, **40(3)**, 4237–4246.

17. Koroleva, M. S., Krasnov, A. G., Senyshyn, A., Schokel, A., Shein, I. R., Vlasov, M. I. and Piir, I. V. (2021) Structure, thermal stability, opto-electronic and electrophysical properties of Mg- and Na-codoped bismuth niobate pyrochlores: Experimental and theoretical study. *Journal of Alloys and Compounds*, **858**, 157742.

18. Gao, L., Liang, K., Liu, Z., Chen, H. and Zhang, J. (2022) Structure dependence of dielectric properties in Ca-doped bismuth magnesium niobate pyrochlores. *Journal of Alloys and Compounds*, **922**, 165859.

19. Koroleva, M. S., Piir, I. V., Zhuravlev, N. A., Denisova, T. A. and Istomina, E. I. (2019) Li- and Mg-codoped bismuth niobate pyrochlores: Synthesis, structure, electrical properties. *Solid State Ionics*, **332**, 34–40.

20. Qasrawi, A. and Mergen, A. (2012) Structural, electrical and dielectric properties of $Bi_{1.5}Zn_{0.92}Nb_{1.5-x}Ta_xO_{6.92}$ pyrochlore ceramics. *Ceramics International*, **38(1)**, 581–587.

21. Du, H. and Yao, X. (2004) Structural trends and dielectric properties of Bi-based pyrchlores. *Journal of Materials Science: Materials in Electronics*, **15**, 613–616.

22. Vugmeister, B. E. and Glinchuk, M. D. (1990) Dipole glass and ferroelectricity in random-site electric dipole systems. *Reviews of Modern Physics*, **62(4)**, 993–1026.